Since January 2020 Elsevier has created a COVID-19 resource centre with free information in English and Mandarin on the novel coronavirus COVID-19. The COVID-19 resource centre is hosted on Elsevier Connect, the company's public news and information website.

Environmental Pollution 288 (2021) 117802

Contents lists available at ScienceDirect

Environmental Pollution

journal homepage: www.elsevier.com/locate/envpol

The impact of COVID-19 lockdowns on surface urban heat island changes and air-quality improvements across 21 major cities in the Middle East☆,☆☆

Ahmed M. El Kenawy [a,b,*], Juan I. Lopez-Moreno [c], Matthew F. McCabe [d], Fernando Domínguez-Castro [e], Dhais Peña-Angulo [c], Islam M. Gaber [f], Abduldaem S. Alqasemi [g], Khalifa M. Al Kindi [a], Talal Al-Awadhi [a], Mohammed E. Hereher [a,h], Sayed M. Robaa [i], Noura Al Nasiri [a], Sergio M. Vicente-Serrano [c]

[a] Department of Geography, Sultan Qaboos University, Al Khoud, Muscat, Oman
[b] Department of Geography, Mansoura University, Mansoura, 35516, Egypt
[c] Instituto Pirenaico de Ecología, Campus de Aula Dei, Avda. Montañana, 50059, Zaragoza, Spain
[d] Division of Biological and Environmental Sciences and Engineering, King Abdullah University of Science and Technology, Thuwal, Saudi Arabia
[e] Aragonese Agency for Research and Development Researcher (ARAID), Department of Geography, University of Zaragoza, Zaragoza, Spain
[f] GIS specialist, Department of Geography, South Valley University, Qena branch, Qena, Egypt
[g] Geography and Urban Sustainability, College of Humanities & Social Science, UAEU, Al-Ain, United Arab Emirates
[h] Department of Environmental Sciences, Faculty of Science, Damietta University, New Damietta, Egypt
[i] Department of Astronomy, Space Science and Meteorology, Faculty of Science, Cairo University, 12613, Egypt

ARTICLE INFO

Keywords:
Air quality
COVID-19
Urban heat island
Climate change
Middle east

ABSTRACT

This study investigates changes in air quality conditions during the restricted COVID-19 lockdown period in 2020 across 21 metropolitan areas in the Middle East and how these relate to surface urban heat island (SUHI) characteristics. Based on satellite observations of atmospheric gases from Sentinel-5, results indicate significant reductions in the levels of atmospheric pollutants, particularly nitrogen dioxide (NO_2), sulfur dioxide (SO_2), and carbon monoxide (CO). Air quality improved significantly during the middle phases of the lockdown (April and May), especially in small metropolitan cities like Amman, Beirut, and Jeddah, while it was less significant in "mega" cities like Cairo, Tehran, and Istanbul. For example, the concentrations of NO_2 in Amman, Beirut, and Jeddah decreased by −56.6%, −43.4%, and −32.3%, respectively, during April 2020, compared to April 2019. Rather, there was a small decrease in NO_2 levels in megacities like Tehran (−0.9%) and Cairo (−3.1%). Notably, during the lockdown period, there was a decrease in the mean intensity of nighttime SUHI, while the mean intensity of daytime SUHI experienced either an increase or a slight decrease across these locations. Together with the Gulf metropolitans (e.g. Kuwait, Dubai, and Muscat), the megacities (e.g. Tehran, Ankara, and Istanbul) exhibited anomalous increases in the intensity of daytime SUHI, which may exceed 2 °C. Statistical relationships were established to explore the association between changes in the mean intensity and the hotspot area in each metropolitan location during the lockdown. The findings indicate that the mean intensity of SUHI and the spatial extension of hotspot areas within each metropolitan had a statistically significant negative relationship, with Pearson's r values generally exceeding - 0.55, especially for daytime SUHI. This negative dependency was evident for both daytime and nighttime SUHI during all months of the lockdown. Our findings demonstrate that the decrease in primary pollutant levels during the lockdown contributed to the decrease in the intensity of nighttime SUHIs in the Middle East, especially in April and May. Changes in the characteristics of SUHIs during the lockdown period should be interpreted in the context of long-term climate change, rather than just the consequence of restrictive measures. This is simply because short-term air quality improvements were insufficient to generate meaningful changes in the region's urban climate.

☆ This paper has been recommended for acceptance by Prof. Pavlos Kassomenos. ☆☆ We declare that all authors have contributed equally to this work, as follows.

* Corresponding author. Department of Geography, Sultan Qaboos University, Al Khoud, Muscat, Oman.
E-mail address: kenawy@mans.edu.eg (A.M. El Kenawy).

https://doi.org/10.1016/j.envpol.2021.117802
Received 11 June 2021; Received in revised form 18 June 2021; Accepted 15 July 2021
Available online 16 July 2021

1. Introduction

Different social, demographic, political and economic processes have contributed to the rapid growth of cities in the Middle East during the past few decades (Costello, 1977). According to the World Bank, the Middle East's urban population increased from 35% in the 1960 to 65% in 2015, far exceeding the global average of 55% (United Nations Population Division, 2018). At the national level, the contribution of the urban population to the total population varied considerably from 35% (Sudan) to 100% (Kuwait) in 2018 (United Nations Population Division, 2018). Currently, the region incorporates some of the most populated urban areas in the world like Greater Cairo, Istanbul, Tehran, Riyadh, and Baghdad. In addition, the region incorporates several city-states, such as Qatar, Bahrain, and Kuwait, which serve as the epicentre of political, economic, and cultural life across its contiguous territory. Due to these rapid urbanization rates, accompanied with inadequate urban resources and services, urbanization has posed several environmental and socioeconomic challenges in many metropolitan areas across the region, including the excessive amounts of greenhouse gas (GHG) emissions, with drastic impacts on the carbon cycle, anthropogenic climate change, air quality, and human health (Nathaniel et al., 2020; Ramahi, 2010; Sibai et al., 2010).

Several studies have referred to the Middle East as a "hotspot" in terms of climate change, with more rapid increases in surface air temperature than the global mean (Diffenbaugh et al., 2007; El Kenawy et al., 2016; Lelieveld et al., 2012; Nasrallah and Balling, 1993). A representative example is Nasrallah and Balling (1993) who reported an increase in air temperature on the order of 0.07 °C/decade over the Middle East from 1945 to 1990, which is higher than the corresponding linear trends for global land areas (0.05 °C/decade). Based on in situ measurements and satellite imagery, a variety of studies have confirmed significant changes in urban climate across the Middle East on a micro-scale (e.g. Abulibdeh, 2021; Abutaleb et al., 2015; Alobaydi et al., 2016; Çiçek and Doğan, 2006; Dihkan et al., 2018; El Kenawy et al., 2020; Elagib, 2011; Karaca et al., 1995; Mohammed et al., 2020; Naserikia et al., 2019). In their assessment of the spatiotemporal characteristics of urban heat island (UHI) in Istanbul, Ünal et al. (2020) demonstrated that the intensity of UHI has increased by 0.41–0.50 °C/decade from 1960 to 2012, compared to 0.13–0.18 °C/decade for daytime UHI intensity. Also, El Kenawy et al. (2020) claimed that surface UHI had expanded significantly over Greater Cairo between 2003 and 2019.

The first case of the Coronavirus disease 2019 (COVID-19) was discovered in China in late 2019 and since then has rapidly spread throughout the entire world (Li et al., 2020). The World Health Organization (WHO) declared the novel coronavirus disease a pandemic on March 11, 2020 (World Health Organization, 2020). The dramatic drop in economic activities during the COVID-19 pandemic, especially during lockdown periods, has provided an once-in-a-lifetime opportunity to investigate the extent to which this pandemic affects urban climate. It is well-established that anthropogenic pollution has considerable influences on air quality and thus heat and energy fluxes in cities (Archer et al., 2020; Jephcote et al., 2021). Nonetheless, these impacts may vary considerably among the different cities, due to their various levels of industrialization, urbanization, and social organization, besides other physical considerations (e.g. geography, climate).

There have been large-scale human activity restrictions during the COVID-19 era to prevent the spread of this disease. Like other parts of the world, several restrictive lockdown measures were implemented in most countries in the Middle East, launching in late March 2020 (Broomandi et al., 2020). These strict preventive lockdown measures included, amongst others, the suspension or significant reductions in catering and entertainment activities, a significant reduction in trade, and small-businesses, cessation of full-time education, as well as directly impacting the work of numerous enterprises. These restrictive measures temporarily reduced the volume of industrial activities and automobile traffic, especially during the first non-working weeks of the pandemic. Alqasemi et al. (2021) demonstrated that, during lockdown periods in 2020, nitrogen dioxide (NO_2) and aerosol optical depth (AOD) concentrations in the northern United Arab of Emirates (UAE) decreased by 23.7% and 3.7%, respectively, compared to the same period in 2019. Also. Ginzburg et al. (2020) indicated that the workload on the Moscow motorway network was roughly four times lower in April 2020 than it was in April 2019. Such preventative measures are likely to impact trends in greenhouse and polluting gases (e.g. NO_2, carbon monoxide [CO], methane [CH_4], and AOD) in urban areas. The improvement in urban air quality due to the COVID-19 pandemic and its associated risk mitigation initiatives has been confirmed at different spatial scales (e.g. Archer et al., 2020; Dantas et al., 2020; Islam et al., 2021; Jephcote et al., 2021; Rodríguez-Urrego and Rodríguez-Urrego, 2020). According to Giani et al. (2020), there was a significant decrease in fine particulate matter ($PM_{2.5}$) over China and Europe by 29.7% and 17.1%, respectively, during the COVID-19 lockdown interventions in 2020. Similarly, within a month of the lockdown, Tobías et al. (2020) noted a reduction of 45, 51, 31, and 19% in PM_{10}, NO_2, SO_2, and CO levels over Barcelona (Spain) within a month of the lockdown. These drastic reductions in GHGs may impact the spatial and temporal characteristics (e.g. intensity, spatial extent) of urban heal heat islands (UHIs). Nonetheless, the response of urban systems to lower GHG emissions can vary significantly from one city to another, depending on population size, urbanization rates, industrialization phases, dominant land use/land cover types, landscape heterogeneity, and physical-human interactions, amongst other driving variables (Yao et al., 2021a).

In the vast majority of the Middle East, the restrictive measures were only in effect for a few weeks, as many countries in the region implemented a gradual return to normal life and, accordingly, GHGs concentrations began to recover a few months after the early restrict lockdown was implemented. This raises the question of whether the short-term improvement in air quality was enough to cause significant changes in climate trends in the Middle Eastern metropolitans, as represented by surface urban heat island (SUHI) intensities and spatial extent, or whether it was merely a transient and temporarily improvement in air quality that failed to influence urban climate trends. What makes this question more interesting is the location of vast areas of the Middle East within the Horse Latitudes, which are characterized by the dominance of high-pressure systems, air subsidence, atmospheric stability, and accordingly intensification of air pollutants (Keikhosravi, 2019; Mohammadpour et al., 2021; Tyrlis et al., 2015). As such, a thorough examination of the unusual situation in 2020 can help answer the most pressing questions about the feasibility of drastic emissions reductions to improve air quality, reduce anthropogenic pressure on urban environments, and mitigate the negative impacts of anthropogenic climate change.

In the pursuit of this objective, the main aims of this study are to (i) assess changes in different pollutant concentrations (e.g. NO_2, CO, CH_4, SO_2, aerosols, and AOD) in 21 metropolitan cities spanning 14 countries across the Middle East during the 2020 COVID-19 lockdown (March–June), and (ii) evaluate their links to the spatial and temporal characteristics (mainly intensity and spatial extent) of SUHI across these metropolitans.

2. Study area

The study incorporates 21 metropolitan areas in the Middle East (Fig. 1). Three sub-groups can be identified among the selected metropolitans. Greater Cairo, Istanbul, Tehran, Greater Khartoum, Ankara, Riyadh, and Baghdad are part of the first group, which includes megacities in the region with total urban agglomeration areas exceeding 1000 km^2 and populations exceeding 5 million. The second group includes states' capitals, such as Amman, Beirut, Doha, Kuwait, Muscat, and Sanaa, which serve as the epicentre of political, economic, and cultural life across their contiguous territory. The last group includes

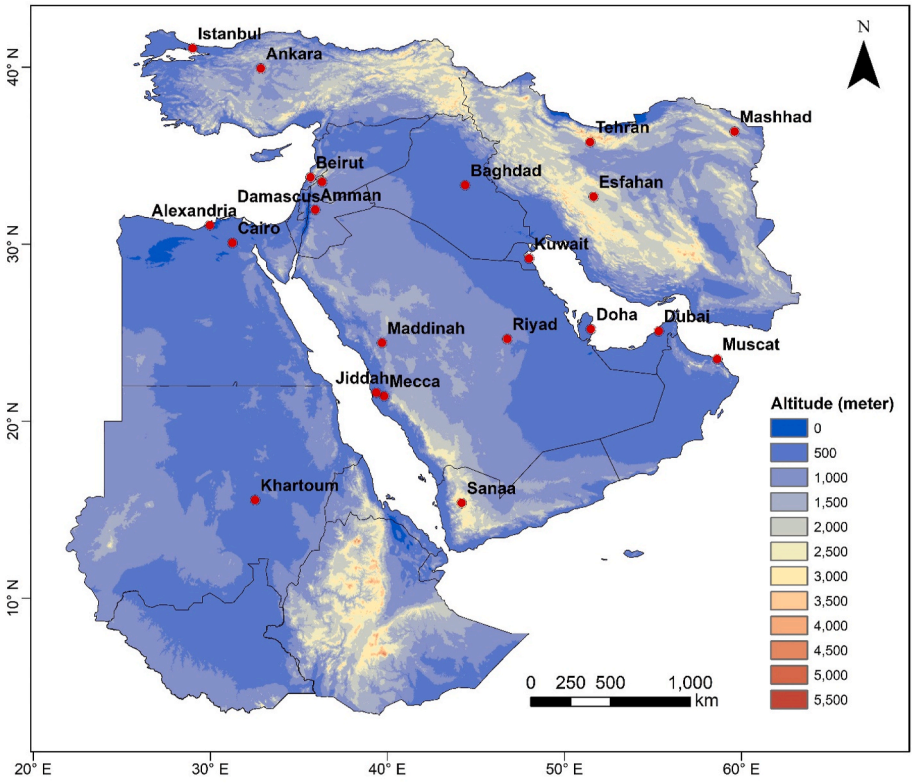

Fig. 1. The selected 21 major metropolitan cities in the Middle East.

some metropolitan areas that have a significant urban center, either because of their economic value (e.g. Alexandria, Jeddah, Mashhad, Esfahan, and Dubai) or due to their religious heritage (e.g. Makkah and Maddinah). For example, with 4–8 million visitors per year, Makkah and Maddinah are extraordinary religious tourism destinations (i.e. Hajj, Umrah, and Ziyarah) for Muslims from all over the world (AL Talib, 2020). Due to its geographical location, broad altitudinal range, and topographical features, the climate of the Middle East is characterized by high variability over space and time. Also, the climate is influenced significantly by both mid-latitude and sub-tropical configurations. As illustrated in Fig. A1., the selected metropolitans exhibit a variety of topographic conditions, ranging between low-altitude cities like Alexandria, Dubai, Jeddah, Muscat, Doha, and Kuwait (altitude is generally less than 30 m above sea level) and highly-elevated cities, such as Sanaa, Esfahan, Tehran, Mashhad, Ankara) (altitude generally exceeds 1000 m a.s.l.). From the climatic perspectives, the selected cities experience varying continental and maritime influences, with inland cities with hybrid continental conditions (e.g. Riyadh and Baghdad), other metropolitans are impacted by maritime influences either from moderate (e.g. Alexandria, Beirut, Istanbul) or tropical (e.g. Jeddah, Doha, Dubai, and Muscat) water bodies. Population size varies considerably amongst the selected metropolitans, with Greater Cairo (>20 million inhabitants) and Istanbul (>15 million inhabitants) representing the most populated cities in the region. Other cities have population size less than one million (e.g. Doha, Kuwait). From a morphological perspective, the selected metropolitans exhibit a wide range of morphological characteristics, with some of them having a compacted circular (e.g. Maddinah and Ankara), longitudinal (e.g. Muscat), latitudinal (e.g. Istanbul, Alexandria) shapes. Also, the total area of the selected metropolitans varies considerably from mega metropolitans like Greater Cairo, Istanbul, Greater Khartoum to small metropolitans (e.g. Maddinah and Makkah, total area less than 150 km^2) (Costello, 1977; Ünal et al., 2020). Amongst all metropolitans, Istanbul ranked first globally in terms of population growth rate in the past few decades, while Cairo ranked eighth (Kennedy et al., 2015).

3. Data and methods

To assess the impacts of city lockdown on air quality, we assessed changes in the composition of the atmosphere in the selected 21 metropolitans during March–June 2020, relative to conditions prior to the lockdown in 2019. Remotely-sensed air quality data for key pollutants, including concentrations of NO, CO, O_3, NO_2, SO_2, and secondary aerosols were obtained for the period March–June for 2019 and 2020. The AOD data were obtained from the Moderate Resolution Imaging Spectroradiometer (MODIS) Version 6 global Multi-Angle Implementation of Atmospheric Correction (MAIAC) (MCD19A2), while data for other atmospheric pollutants (i.e. NO_2, O_3, SO_2, CO, and aerosols) were provided by the European Space Agency (ESA) Sentinel-5 precursor (also known as Sentinel-5p) TROPOMI (Tropospheric Monitoring Instrument) mission (Veefkind et al., 2012). Sentinel-5P is the first Copernicus mission to monitor the atmosphere, with the goal of narrowing the data gap between the launch of Envisat satellites (especially the SCIAMACHY instruments) and Sentinel-5 (Veefkind et al., 2012). Sentinel-5P is a near-polar orbiting sun-synchronous satellite positioned at an altitude of 817 km in an ascending node with an equator crossing time at 13:30 (local time) (Zheng et al., 2019). The satellite is equipped with the most advanced TROPOMI instrument for measuring ultraviolet–visible (270–500 nm), near-infrared (675–775 nm), and short-wave infrared (2305–2385 nm) spectral bands, allowing to image different atmospheric pollutants at improved accuracy, compared with other satellites (Veefkind et al., 2012). Sentinel-5 provides a quality band, with values ranging from 0 (poor) to 1 (excellent), which is important for pixel filtering and data quality verification (e.g. elimination of cloud interference). Overall, air quality data were extracted for the metropolitan areas on a monthly scale for the period March–June between 2019 and 2020 and at a grid resolution of 7 × 3.5 km.

In an attempt to provide a complete picture of the state of air quality

in the 21 metropolitans during the restricted lockdown period (March–June 2020), we proposed a ranking score for each atmospheric pollutant. Specifically, the anomalies of a particular pollutant in the 21 metropolitans in 2020, computed with respect to those of 2019, were ranked in ascending order for each month during the lockdown period, with the metropolitan with the most anomalous negative values (i.e. higher improvement) ranked first, and the metropolitan with the highest positive anomaly (i.e. least improvement) ranked 21st. Then, for this month, we defined the score (S) of this pollutant, as:

$$S = \frac{seq_i - 1}{c - 1} \ldots \quad (1)$$

where *seq* is the sequence number of each metropolitan and *c* is the total count of the metropolitans (*N=21*). According to this methodology, a score was computed for each atmospheric pollutant on a monthly basis (i.e. for March, April, May, and June 2020). The four scores for each atmospheric pollutant were then averaged to get the overall score of every pollutant during the lockdown period. Finally, we calculated an air quality aggregated index to summarize the whole picture of air quality in each city, which takes into account the scores of the six pollutants employed in this study. This index was computed for each metropolitan using an average of the scores of the six pollutants for this metropolitan. Simply, the air quality aggregated index values range from 0 (least improved air quality) to 1 (most improved air quality).

To characterize SUHI during the COVID-19 lockdown period across the selected metropolitan areas in the Middle East, land surface temperature (LST) was employed as an indicator of land surface physical processes. Satellite observations have provided many useful and powerful databases for evaluating the dynamics of SUHI. Specifically, Thermal Infrared Spectrometer (TIR) imagery can provide a large-scale and simultaneous view of LST data at a relatively detailed spatial scale and for regular and continuous time intervals, with a positive cost–benefit ratio. The full archive of the 8-day composites of the LST product (MYD11A2V.6) (https://lpdaac.usgs.gov/) spanning March–June period between 2003 and 2020 was employed in this study (de Andrade et al., 2021). Specifically, we retrieved daytime (1:30 p.m.) and nighttime (1:30 a.m.) LST from the Aqua satellite (MYD11A2 V.6) at a 1 km grid resolution for the selected 21 metropolitans in the Middle East. This study characterized SUHI using both daytime and nighttime LST, allowing for a more detailed view of SUHI diurnal variations. Also, under different levels of restrictive measures between day and night hours, this approach allows characterizing the varying responses of daytime and nighttime SUHI to COVID-19 lockdown. MOD11A2 has been corrected for atmospheric effects (e.g. clouds, aerosols), resulting in high-quality data (Tonooka, 2005). As such, it has been increasingly employed to assess SUHI intensity and spatial extension, as well as its temporal changes and driving forces, across many cities in the world (e.g. Imhoff et al., 2010; Li et al., 2017; Meng et al., 2018; Yao et al., 2017, 2018; Li et al., 2021), including the Middle East (e.g. El Kenawy et al., 2020; Nassar et al., 2016).

The intensity of SUHI is determined based on the concept of "local climate zones". Specifically, from 2003 to 2020, we identified the hot and cold spot regions for each month separately. Then, the SUHI intensity was computed as the spatially-averaged LST temperature difference between these two thermally-distinct areas in each metropolitan (i.e. the hotspot and cold spot). Different approaches have been used to delineate hot and cold urban spots in the literature, including numerical classification, Gaussian surface fitting, radial sampling, and hotspot methods (Zhou et al., 2018; Huang and Wang, 2019). Amongst them, hotspot methods (e.g. spatial autocorrelation, spatial clustering) are commonly used to delineate hotspot regions in urban agglomerations. However, these hotspot methods focus more on the spatial perspective of SUHI, with less attention paid to how it evolves over time, which is extremely important given that cities rapidly change over time and their local climate is also highly variable. Accordingly, to account for the dynamical evolution of SUHI over time and space, we applied the algorithm proposed by (El Kenawy et al., 2020). According to this methodology, a spatial anomaly of daytime (nighttime) LST at each time step (8-day composite) for each grid within a metropolitan was computed, as follows:

$$LST_{anomaly=LST_i-\mu} \ldots \quad (2)$$

where *LSTi* refers to daytime (nighttime) *LST* at grid *i* at a given time step, while μ indicates the average of daytime (nighttime) LST across all grids within the metropolitan at the same time step. Then, these 8-day anomalies were aggregated on a monthly basis. To define the spatial extent of the most anomalous "hotspot" and "cold spot" across each metropolitan and for a particular month within the period 2003–2020, the grid (i) was assigned to the most anomalous hotspot when:

$$LST_{anomalyforgridi} > 0.5(Q75_{forallgrids} - Q25_{forallgrids}) + Q75_{for\ all\ grids} \ldots \quad (3)$$

Alternatively, the grid is assigned to the most anomalous cold spot when:

$$LST_{anomalyforgridi} < Q25_{forallgrids} - 0.5(Q75_{forallgrids} - Q25_{forallgrids}) \ldots \quad (4)$$

Following Equations (2) and (3), *Q75* refers to the value of the 75th percentile calculated for all LST anomalies for all grids at a given time step, while *Q25* denotes the value of the 25th percentile. Based on these equations, each grid within the metropolitan area will be assigned to the most anomalous hotspot if it meets the conditions of Equation (2), and to the most anomalous cold spot if it fulfills the requirement of Equation (3). Other grids in the metropolitan area will refer to transitional thermal zones between the most anomalous hot and cold spots. Based on LST spatial anomaly, the applied algorithm allowed to determine the portions of the metropolitan area with higher (hotspot) and colder (cold spot) surface temperature in a comparable manner over both space and time. Here, it should be noted that while our approach to delineate SUHI relies primarily on LST differences to distinguish hot and cold spots within each metropolitan area, this definition indirectly accounts for the difference between urban and rural areas. Basically, our definition is based on the assumption that the most anomalous hotspots in any metropolitan area are likely to be located in most urbanized areas, where built-up areas, population densities, green space ratio, and dominant economic activities are more evenly distributed (Wu et al., 2020). The anomalous cold spot, on the other hand, is mostly found in less-urbanized and sub-urban areas. Further details about this method is outlined in El Kenawy et al. (2016).

After calculating the intensity and spatial coverage of SUHI for each month from 2003 to 2020, we first compared the values of SUHI intensity and total area for the lockdown months in 2020 (i.e. March–June) with their long-term (2003–3019) averages. Second, we compared the difference between the value of SUHI intensity/spatial coverage in 2020 and the average of these metrics over the same months in 2019. Calculating SUHI metrics relative to both long-term (2003–2019) and short-term (i.e. 2019) base periods allows determining whether changes in SUHI metrics reflect abrupt changes associated with the short-term improvement in air quality due to GHGs deductions after COVID-19 lockdown or merely a phase of long-term natural climate change. Finally, the Pearson correlation coefficient was used to assess the association between changes in the mean intensity of SUHI and the corresponding spatial coverage of hotspot area using the short-term (i.e. 2019) and long-term (2003–2019) anomaly. This association statistic was also employed to explore the dependency between changes in air pollutants and SUHI characteristics (i.e. intensity, spatial coverage) for the period 2019–2020. Statistical significance of correlation was assessed at the 95% level ($p < 0.5$).

4. Results

4.1. Changes in air quality during lockdown

Fig. 2 illustrates changes (%) in the amounts of the different atmospheric pollutants during the lockdown period (March–June 2020), as compared to their averages for the same period in 2019, while their averages for the 21 metropolitans are listed in Table 1. Monthly changes were calculated separately. A rise in the amount of AOD was noted for almost all metropolitans in March, with values ranging between 3.6% (Muscat) and 75% (Maddinah). Exceptionally, only two metropolitan areas, Kuwait (−12%) and Mashhad (−10%), showed a decrease in AOD. In April, almost half of the metropolitans experienced an increase in AOD concentrations, while the other half witnessed a decline. Notably, almost all positive anomalies were found inland, with the largest increase found in Baghdad (79.7%), Mashhad (53.5%), Tehran (53.3%), and Cairo (33.3%). Rather, coastal metropolitans exhibited the most pronounced negative changes in AOD, including Beirut (−29.5%), Jeddah (−38.4%), and Alexandria (−28.5%). In May, there was a noticeable improvement in AOD concentrations, with metropolitans either experiencing a strong negative anomaly like Isfahan (−19.1%), Muscat (−15%), Cairo (−14.5%), Amman (−14.1%), Jeddah (−11%), and Baghdad (−10.1%) or witnessing a slight increase like Maddinah (0.2%), Khartoum (2%), and Damascus (3.9%). In June, there was a significant reduction in AOD levels in several metropolitan areas. This was apparently the case for Beirut, Makkah, Jeddah, Cairo, and Maddinah. Comparing the monthly relative anomalies of AOD across metropolitans, it can be seen that aside from March, when the restrictive measures were applied too late in most countries in the region, AOD decreased in each month (i.e. April to June). Nonetheless, Doha, Baghdad, and Tehran all showed the least improvement in AOD concentrations during the lockdown period.

Aerosols exhibited a general decrease in their levels, especially in May. The most drastic reductions were found in metropolitans of hyper-arid zones, characterized by vast neighbouring deserts, like Amman (−282.2%), Cairo (−208.2%), Muscat (−180.2%), Khartoum (−144%), Dubai (−119.9%), and Baghdad (−98.7%). In few exceptions, there was an increase in aerosol concentrations (e.g. Alexandria (529.9%), Damascus (121%), and Tehran (73.5%)). In June, aerosol concentrations showed less differences with June 2019, with variations ranging between −24.3% (Kuwait) and 58.7% (Amman). The most anomalous changes in aerosol concentrations in June were found in Muscat (394.9%), Damascus (−177%), Baghdad (−171.1%), and Sanaa (116.1%).

In contrast to AOD and aerosol concentrations, a major increase in CO levels occurred in most of the metropolitans during March and May. Majority of these metropolises are located in the Arabian Peninsula, such as Sanaa (11.8% and 9.1% in March and April, respectively), Doha (5.6% and 6.3% in March and May, respectively), Riyadh (4.9% and 3.9% in March and May, respectively), Jeddah (6.1% and 6% in March and May, respectively), and Dubai (5.6% and 2% in March and May, respectively). More metropolitans (e.g. Doha, Kuwait, and Sanaa) and beyond (e.g. Amman, Esfahan, Baghdad, Beirut, Damascus, Tehran, Mashhad) showed a decline in CO concentrations in June. Nevertheless, this improvement was slightly weak (generally less than 3%). Only five metropolitans, including Alexandria, Dubai, Khartoum, Maddinah, and

Table 1
Changes (%) in the concentrations of air pollutants, averaged for the selected 21 metropolitans in the Middle East. Changes were computed as the differences between air pollutants levels in 2020 and those of 2019. Differences were computed for each month independently during the lockdown period (i.e. March–June).

	March	April	May	June
AOD	25.71	4.78	−0.20	−2.58
Aerosols	−0.15	29.92	−39.63	4.82
CO	3.27	0.79	4.05	−0.30
NO_2	11.18	−10.28	−19.72	19.43
O_3	25.42	4.70	−0.90	−3.17
SO_2	18.54	8.52	7.82	16.44

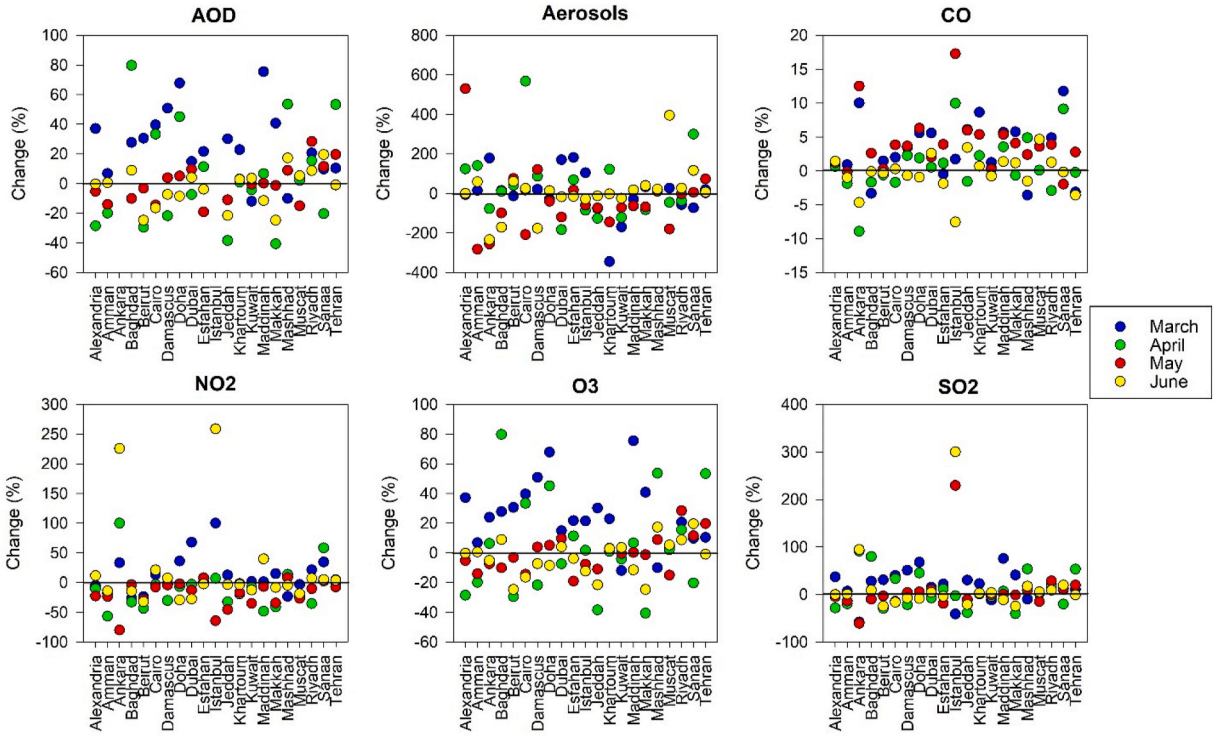

Fig. 2. Changes (%) in the concentrations of air pollutants, calculated as the differences between these concentrations in 2020 and those of 2019. Differences were computed for each month independently during the lockdown period (i.e. March–June).

Muscat, had CO levels rise during the entire lockdown period.

The concentrations of NO_2 decreased significantly during the lockdown period, with the largest changes occurred in April and May, given that 18 metropolitans had lower NO_2 levels than in 2019. The most NO_2 reductions in April occurred in Amman (−56.6%), Maddinah (−48.3%), Beirut (−43.4%), Makkah (−41.1%), Riyadh (−35.6%), Baghdad (−32.9%), Jeddah (−32.3%), and Damascus (−30.3%). Notably, improvement in NO_2 levels was less significant in the most populated metropolitans, especially Cairo (−3.1%) and Tehran (−0.9%), besides the Gulf cities (e.g. Dubai, Doha, and Kuwait). Five metropolitans exhibited reductions in NO_2 concentrations in all months of the lockdown, including Amman, Baghdad, Beirut, Khartoum, and Muscat. Rather, Sanaa was the only metropolitan that witnessed NO2 levels increase during the lockdown.

Fig. 2 illustrates how much O_3 was impacted during the lockdown period. Only two metropolitans (Kuwait and Mashhad) exhibited a decrease in O_3 levels in March. Other metropolitans showed an increase, with values ranging from 3.6% (Muscat) to 75.4% (Mashhad). O_3 levels appeared to show two distinct patterns during the lockdown. O_3 levels declined in the metropolitans of the Arabian Peninsula (i.e. Makkah, Jeddah, and Sanaa) and the Mediterranean (i.e. Alexandria and Beirut). The greatest reductions were found in Makkah (−40.6%), Jeddah (−38.4%), and Beirut (−29.5%). A second pattern characterized by an increase in O_3 concentrations in April was noted in the region megacities, including Cairo (33.3%), Tehran (53.3%), Baghdad (79.7%), and Riyadh (15.5%), as well as Doha (45%). In most metropolitans, O_3 levels showed less differences in May 2020 than they had in 2019. Esfahan (−19.1%), Muscat (−15%), and Cairo (−14.5%) experienced the greatest improvements in O_3, while a rapid increase was noted in Riyadh (28.4%), Tehran (19.6%), and Sanaa (11.5%). In June, many metropolitans experienced either a decrease in O_3 levels (e.g. Beirut, Makkah, Jeddah, and Cairo) or a slight increase (usually less than 5%). Only Riyadh and Khartoum displayed an increase in O_3 concentrations in the whole lockdown period, although this increase was much stronger in Riyadh (8.8 ± 28.4%) than in Khartoum (1 ± 22.9%).

In March 2020, the majority of the metropolitans showed an increase in SO_2 levels. Exceptionally, Ankara, Istanbul, Kuwait, and Mashhad showed significant reductions on the order of −58%, −41.2%, −12.1%, and −12%, respectively. In April, megacities such as Ankara, Baghdad, Tehran, Cairo, and Riyadh exhibited the greatest SO_2 increases, with concentrations reaching 90.9%, 79.7%, 53.3%, 33.3%, and 15.5%, respectively. Apart from Istanbul (−2.8%), the decrease in SO_2 concentrations was more noticeable in small metropolises, such as Makkah, Dubai, and Kuwait, or in the Mediterranean metropolises, such as Alexandria and Beirut. In some of the most densely populated metropolises, such as Ankara (−61%), Esfahan (−19.1%), Cairo (−14.5%), and Baghdad (−10.1%), the situation improved in May. In June, an increase in SO_2 levels occurred in the region's most populous cities, including Istanbul (300%), Ankara (94.3%), Baghdad (9%), and Riyadh (8.8%). In addition to Cairo (−16.5%), the reductions in SO2 were noticeable in smaller cities, such as Beirut and Makkah (−24.7%), Maddinah (−11.5%), and Doha (−8.6%). Khartoum and Riyadh were the only metropolitan areas whose SO_2 levels increased throughout the entire lockdown period.

Fig. 3 depicts the atmospheric pollutant scores, which show how each pollutant performed in the lockdown period (March–June 2020). The overall state of air quality for each metropolitan area is also shown using an aggregated index. Air quality in Amman, Beirut, Jeddah, and Kuwait improved during the lockdown, with index values generally above 0.7. Conversely, in this situation, the cities that showed less improvement in air quality were Sanaa (0.38), Doha (0.41), Riyadh (0.41), Mashhad (0.44), and Tehran (0.47). CO, NO_2, and O_3 reductions, with 0.93, 0.90, and 0.78 value scores, respectively, led to Amman's significant improvement in air quality. For Beirut, decreasing levels of NO_2, SO_2, O_3, and CO were mainly responsible for the improvement in air quality. A decrease in aerosol concentrations (score values of 0.90 and 0.88) helped in improving air quality in Kuwait and Jeddah. The primary driver of better air quality in Makkah and Muscat was the reduction in NO_2, O_3, and SO_2 levels. On the other hand, the decline in air quality in Sanaa was caused by an increase in the majority of pollutants, especially NO2 (score = 0.18) and aerosols (score = 0.34). Due to an increase in AOD, O_3, and SO_2, the quality of the air in Doha was reduced during the lockdown months.

For the big metropolitan areas in the region, NO_2 was the most degraded atmospheric pollutant during the COVID-19 lockdown, with value scores of 0.4 or lower. Rather, the most significant improvement occurred in CO, especially for Tehran (score = 0.83) and Cairo (score = 0.63). We noticed significant differences between the Gulf metropolitans. Kuwait and Muscat showed improvements in their air quality during the lockdown, mainly due to a decrease in NO_2, O_3, and SO_2. Conversely, Doha and Dubai showed less improvement in their air quality, with index values of 0.41 and 0.51, respectively. The levels of atmospheric pollutants in these cities, especially CO, O_3, NO_2, and SO_2, were higher during the lockdown than they were in 2019.

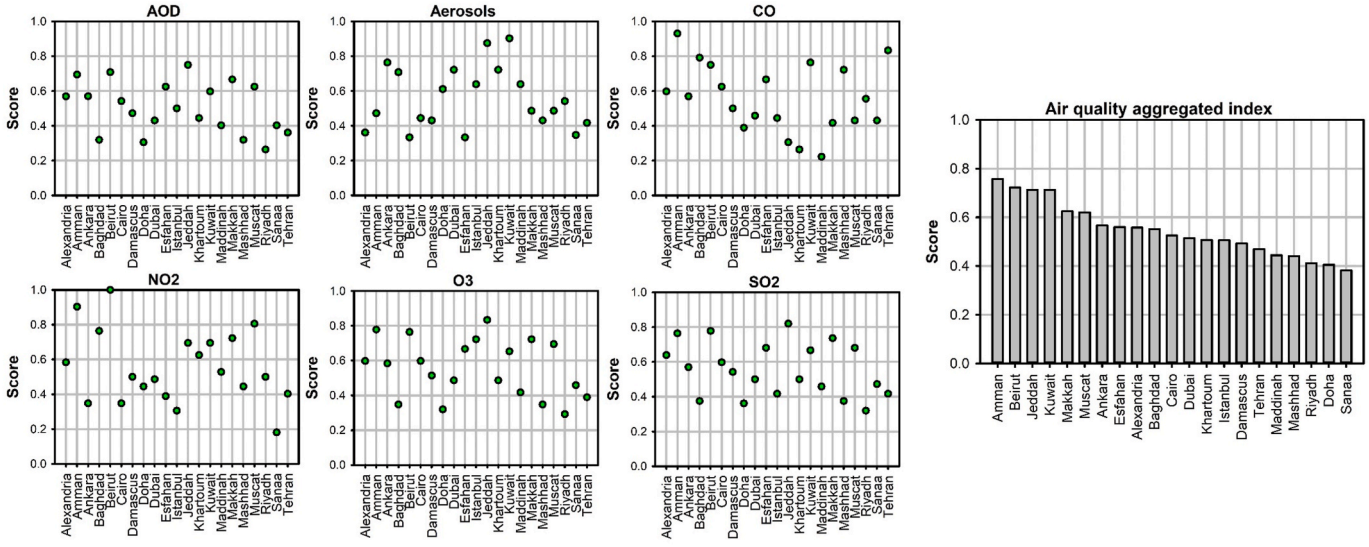

Fig. 3. Ranking the 21 metropolitans according to the score computed for each atmospheric pollutant. The right panel indicates the air quality aggregated index accounting for the full range of atmospheric pollutants.

4.2. Changes in the mean intensity of SUHIs during lockdown

Fig. 4 illustrates changes in the mean intensity of SUHI over the 21 metropolises, as compared to that for the long-term (2003–2019) average. Results are presented for both daytime and nighttime SUHIs. As depicted, nighttime SUHI intensity declined drastically in March, with values ranging between −1.16 °C in Cairo and 0.02 °C in Jeddah. Only two metropolitans, Khartoum (0.03 °C) and Mashhad (0.04 °C) witnessed an increase in their nighttime SUHI intensity. Fig. 4 informs that March's largest decrease in mean intensity of nighttime SUHI occurred in the megacities, including Cairo (−1.16 °C), Tehran (−0.94 °C), Baghdad (−0.67 °C), Istanbul (−0.65 °C), and Riyadh (−0.52 °C). This decrease was also noted in Dubai (−0.91 °C) and Alexandria (−0.78 °C). Also, daytime SUHI was dominated by a decreasing mean intensity. Nonetheless, the mean intensity of daytime SUHI in Jeddah, Doha, Istanbul, Tehran, Esfahan, and Khartoum was higher than nighttime SUHI. Khartoum, Esfahan, Tehran, and Istanbul all recorded the highest (>1 °C) mean intensity of daytime SUHI, compared to the period 2003–2019. Nighttime SUHI intensity had a smaller decrease than daytime SUHI in April, with a mean intensity change of 0.03 °C (Jeddah and Riyadh) to 2.97 °C. (Tehran). Again, megacities like Tehran (2.97 °C), Ankara (2.89 °C), and Istanbul (1.97 °C) had the largest increases in daytime SUHI mean intensity. In contrast, the largest decrease in the mean intensity of daytime SUHI was found in smaller metropolitans like Makkah and Maddinah, as well as the Mediterranean metropolitans like Alexandria, Damascus, and Beirut. In May, the mean intensity of daytime SUHI increased across the Arabian Peninsula and the Gulf region, including Sanaa (2.7 °C), Doha (0.42 °C), Kuwait (0.37 °C), Dubai (0.36 °C), and Riyadh (0.24 °C), as well as some megacities like Istanbul (1.5 °C) and Tehran (0.78 °C). Conversely, the largest decrease in daytime SUHI was observed in Cairo, Damascus, Amman, and Baghdad, which were all 0.75–1.18 °C cooler. Dubai, Beirut, Maddinah, and Cairo metropolitans experienced the most notable reductions in the intensity of their nighttime SUHIs, with differences less than 0.6 °C (e.g. Baghdad, Ankara, and Jeddah). Daytime and nighttime SUHI patterns had similar differences in June, however, with less differences than in May.

A closer look at Fig. 4 reveals some interesting results. First, during the lockdown of 2020, the intensity of SUHI decreased generally in most metropolitans, which was accompanied by a higher change in the mean intensity of SUHI during nighttime than during daytime. Second, the reduction was more pronounced in smaller metropolises (e.g. Amman, Makkah, Maddinah, and Beirut). Third, SUHI intensity decreased more over the middle phase of the lockdown, rather than when it began (March) or ended (June). Fourth, during the entire period of lockdown, only Cairo (the largest city in the region) had a decrease in mean intensity for both daytime and nighttime SUHI. Lastly, all Gulf's metropolitans, with the exception of Muscat, had an increase in the mean SUHI intensity during the day, but a decrease during nighttime.

Fig. 5 shows the evolution of the mean intensity of SUHI in the lockdown period, but as compared with the same period in 2019. Similar to results from the long-term (2003–2019) period. The findings show that the mean intensity declined more noticeably in the majority of the metropolitans during the nighttime, especially between March and May. Even so, it appears that changes in SUHI intensities, which were generally positive, were much stronger during daytime than in nighttime. The rapid increase in the mean intensity of daytime SUHI occurred in the megacities of Tehran and Ankara in April, being stronger for some

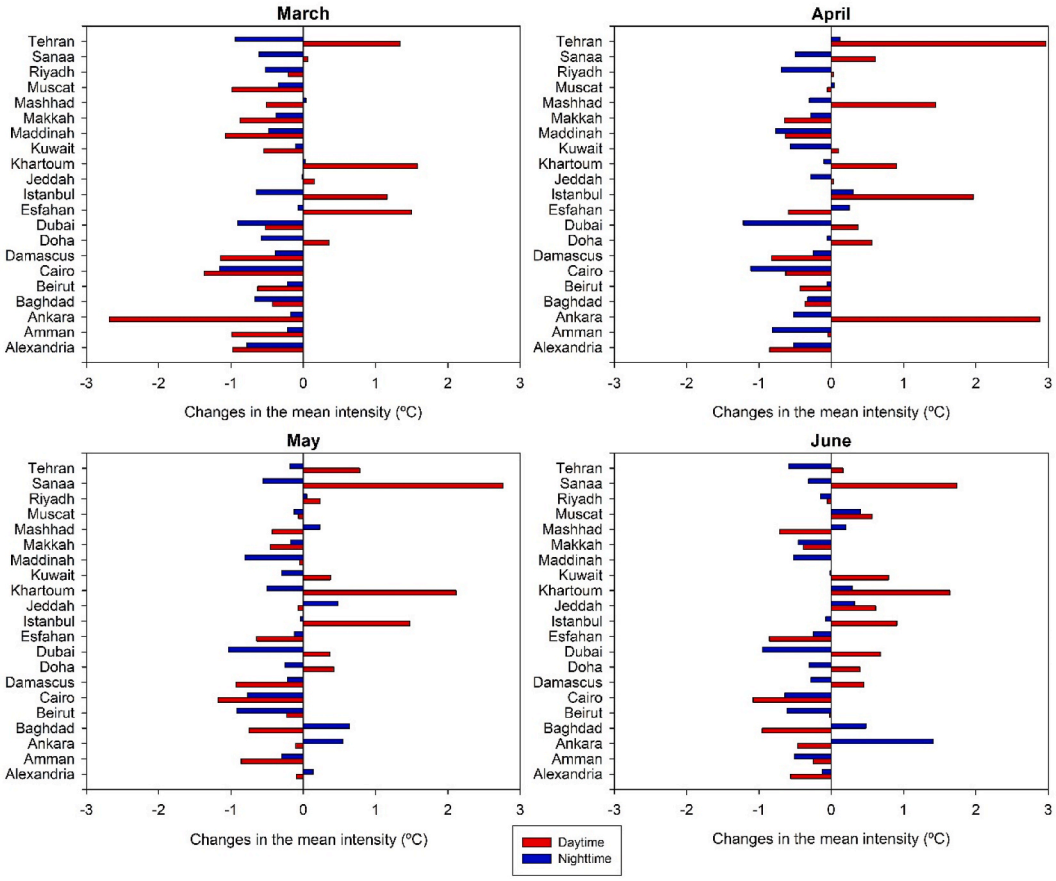

Fig. 4. Anomalies of the mean intensity of daytime (red) and nighttime (blue) SUHI during the 2020 lockdown months, relative to those computed for the longer base period of 2003–2019. Anomalies were computed for each month independently. (For interpretation of the references to colour in this figure legend, the reader is referred to the Web version of this article.)

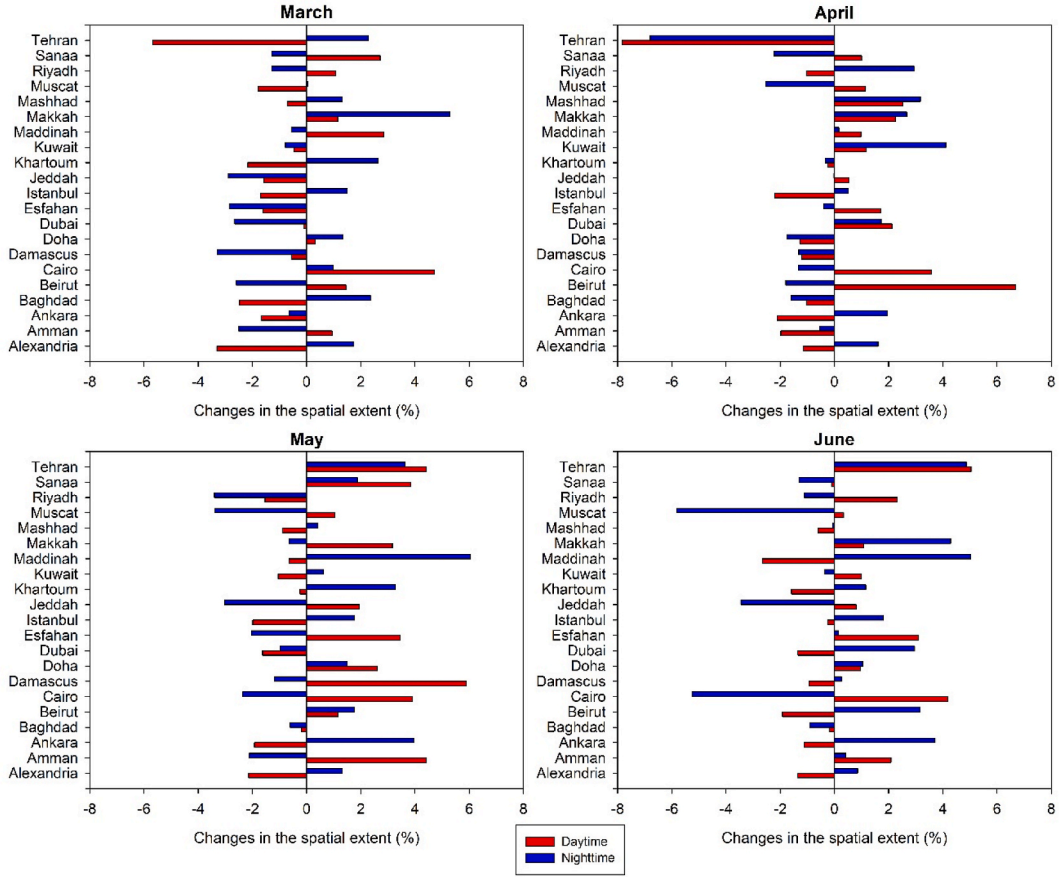

Fig. 5. Anomalies of the spatial extent of hotspot areas during daytime (red) and nighttime (blue) in the 2020 lockdown months, relative to those computed for the longer base period 2003–2019. Anomalies were computed for each month independently. (For interpretation of the references to colour in this figure legend, the reader is referred to the Web version of this article.)

cities in the Arabian Peninsula like Sanaa and Maddinah and the Gulf countries (e.g. Kuwait, Dubai, and Doha) in May and June. A comparison of Figs. 4 and 5 reveals that short-term anomalies (i.e. relative to 2019) in the mean intensity were lower than those based on long-term anomalies (i.e. 2003-2019). Notably, daytime and nighttime mean SUHI changed little (almost less than 0.5 °C) during the lockdown year 2020, relative to the same period in 2019, especially for daytime. Rather, the long-term anomalies suggested larger differences (0.5–1 °C for nighttime and 1–1.5 °C for daytime, on average).

4.3. Changes in the spatial extent of SUHIs during lockdown

Fig. 6 illustrates how the total hotspot area in each metropolitan area changed during the 2020 lockdown, compared to their averages from 2003 to 2019. In March, daytime hotspots areas decreased in 13 out of 21 metropolises, with values between −0.12% (Dubai) and −5.68% (Tehran). Rather, during the day, the hotspot area increased in several metropolitan areas, including Cairo (4.71%), Maddinah (2.85%), Beirut (1.45%), Makkah (1.15%), and Amman (0.94%), among others. During the night, a similar pattern was observed, but with notable increases in megacity hotspots, such as Cairo (0.98%), Istanbul (1.49%), Tehran (2.7%), and Baghdad" (2.36%). Major cities across the Arabian Peninsula (e.g. Sanaa, Makkah, Maddinah, and Jeddah) and the Gulf region (e.g. Kuwait, Muscat, and Dubai) experienced an increase in both daytime and nighttime hotspots in April. Kuwait and Riyadh had the largest increase in daytime hotspot areas, with values of 4.11% and 2.94%, respectively. In Tehran, on the other hand, the total area of hotspots fell dramatically during day (−7.83%) and night (−6.80%). The hotspots in Beirut, Doha, Sanaa, and Tehran increased during day and at night in May, albeit with a greater increase during daytime. In contrast, hotspots decreased at both day and nighttime in Baghdad and Riyadh. In contrast, the metropolitans of the Arabian Peninsula (e.g. Riyadh, Jeddah, and Makkah) and the Gulf region (e.g. Muscat and Dubai) had the greatest reduction in their nighttime hotspots. With the exception of Cairo (−2.35%), other megacities like Ankara (3.97%), Tehran (3.64%), and Istanbul (1.77%) demonstrated the most significant growth in the total nighttime hotspot area. Overall, albeit with the differences in the sign of change (i.e. increase/decrease) in the total hotspot area during the lockdown months, we observed two distinct patterns: more rapidly changes in the daytime hotspots in megacities like Cairo, Tehran, and Istanbul and, instead, stronger changes in nighttime hotspots in less-populated and small metropolitans like Doha, Makkah, Muscat, and Kuwait.

Fig. A2 depicts changes in the area of hotspots during the months of the 2020 lockdown, as compared to the same period in 2019. The majority of the metropolitans showed an increase in both the daytime and nighttime SUHI hotspots, being much stronger in May. Nonetheless, this increase was more pronounced during daytime, particularly for small metropolises like Makkah (2.81%), Sanaa (1.84%), Jeddah (1.30%), Muscat (1%), Doha (0.84%), and Beirut (0.79%). Regardless of the sign of change (i.e. positive or negative), the Arabian Peninsula and the Gulf metropolitans had higher hotspot change rates, especially for Maddinah, Sanaa, Dubai, and Makkah during daytime. On the other hand, for megacities, like Tehran, Cairo, Istanbul, Tehran, Ankara, and Riyadh, these changes were almost negligible. An inspection of Fig. 6 and A2 reveals that changes in the hotspot areas during the lockdown were much smaller when considered short-term (i.e. 2019) anomaly than those based on the long-term (2003–2019) anomaly. Fig. A2 indicates

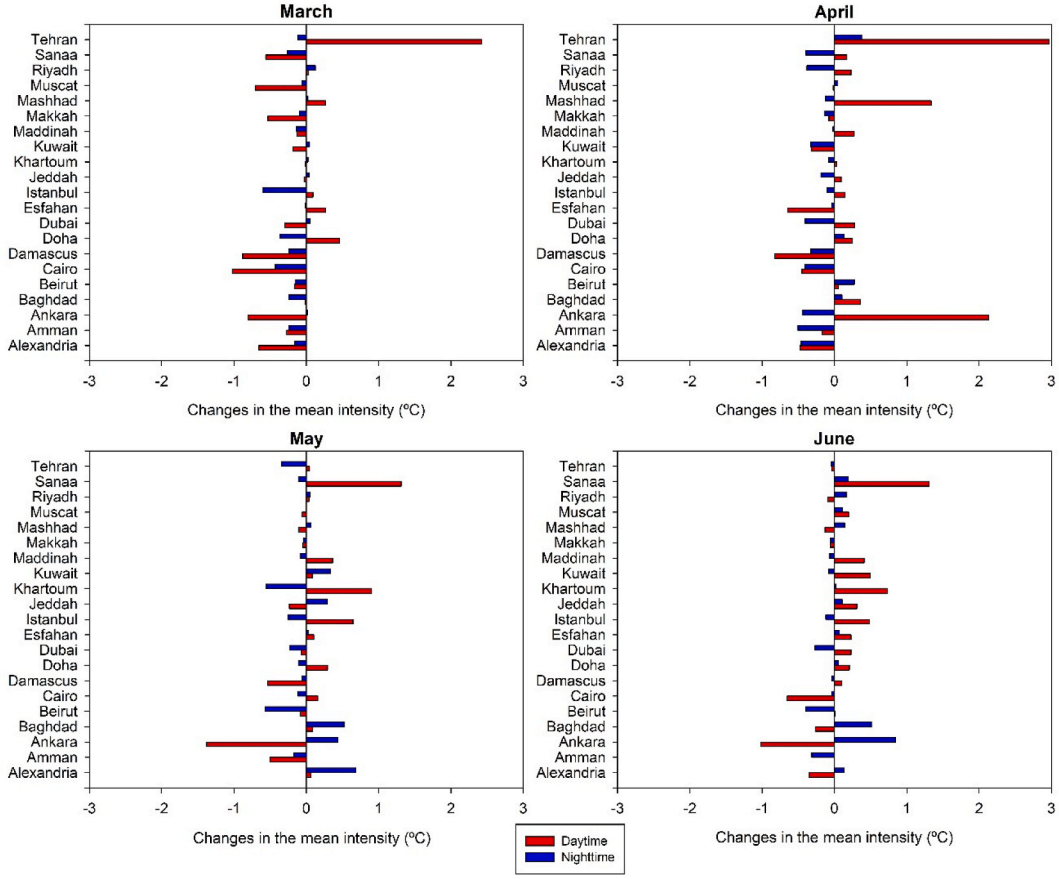

Fig. 6. Anomalies of the mean intensity of daytime (red) and nighttime (blue) SUHI during the 2020 lockdown months, relative to those of 2019. Anomalies were computed for each month independently. (For interpretation of the references to colour in this figure legend, the reader is referred to the Web version of this article.)

that hotspot changes rarely exceed 2% either for daytime or nighttime, with the exception of the metropolises of the Arabian Peninsula and the Gulf region.

Fig. 7 shows the relationship (agreement) between changes in the mean intensity of daytime and nighttime SUHI during the lockdown and the corresponding changes in the spatial extent of hotspot areas. Herein, changes were computed with respect to the near-term (2019) and long-term (2003–2019) periods. Regardless of the base period to calculate the anomalies, the majority of the metropolitans showed a negative relationship between SUHI mean intensity and the total area of hotspots. When SUHI mean intensity increased, the total area of hotspot decreased and vice versa. This dependency was evident for all months of the lockdown, as well as both daytime and nighttime. Nevertheless, this association was much stronger in April, though being statistically non-significant during nighttime ($r = 0.37$, $p > 0.05$). Additionally, when considering the short-term anomaly, results also show a negative correlation between the mean intensity of SUHI and the corresponding hotspot area. However, this association was notably stronger and statistically significant ($p < 0.05$) for daytime SUHI, especially in March, April, and June.

5. Discussion

Our study assessed changes in the concentrations of a number of air pollutants (e.g. AOD, aerosols, CO, O_3, NO_2, and SO_2) and SUHI characteristics over 21 metropolitan cities in the Middle East during the 2020 restricted lockdown (March–June). Air quality was characterized based on satellite-derived air pollution retrievals from Sentinel-5 for the period 2019–2020. Although actual measured data are highly desired as they provide a "real" estimation of the state of air quality using ground measurements, the uneven distribution of these stations makes it difficult to assess air quality conditions using these data sources. However, air quality data from Sentinel-5 have proven to be effective tools for characterizing air quality in different regions in the Middle East (e.g. Alqasemi et al., 2021; El-Nadry et al., 2019; Safarianzengir et al., 2020) and worldwide (e.g. Gautam, 2020a,b; Hashim et al., 2021; Jephcote et al., 2021; Li et al., 2020; Naqvi et al., 2021; Shehzad et al., 2020; Stratoulias and Nuthammachot, 2020). Overall, based on Sentinel-5 data, our findings demonstrate the expectation that there would be significant reductions in the levels of air pollutants during the lockdown period, particularly in April and May. The reductions were mostly in NO_2, SO_2 and O_3, and to a lesser extent in AOD and aerosols. This finding concurs with a wide range of recent regional (e.g. Alqasemi et al., 2021; Broomandi et al., 2020) and global (e.g. Aman et al., 2020; Broomandi et al., 2020; Chen et al., 2020; Rodríguez-Urrego and Rodríguez-Urrego, 2020) studies that evidence the dependency between air quality and COVID-19 lockdown. For example, Alqasemi et al. (2021) reported a decrease in NO_2 (23.7%) in the northern UAE during the period of April–June 2020, as compared to the same period in 2019. Also, Broomandi et al. (2020) noted a decline in SO_2 and NO_2 levels and conversely an in increase in AOD in Tehran between 21st March to April 21, 2020. Based on in situ measurements, Aman et al. (2020) indicated a significant improvement in the levels of NO_2, $PM_{2.5}$, and PM_{10} in Ahmedabad (India) during COVID-19 lockdown.

Notably, our study indicates that the positive influence of the pandemic lockdown on air quality was more significant in small metropolitans rather than in megacities of the region. Based on an aggregated air quality index, it was evident that air quality improved in small metropolitans like Amman, Beirut, Jeddah, Kuwait, Makkah, and Muscat, while it was less impacted in the largest and most populated

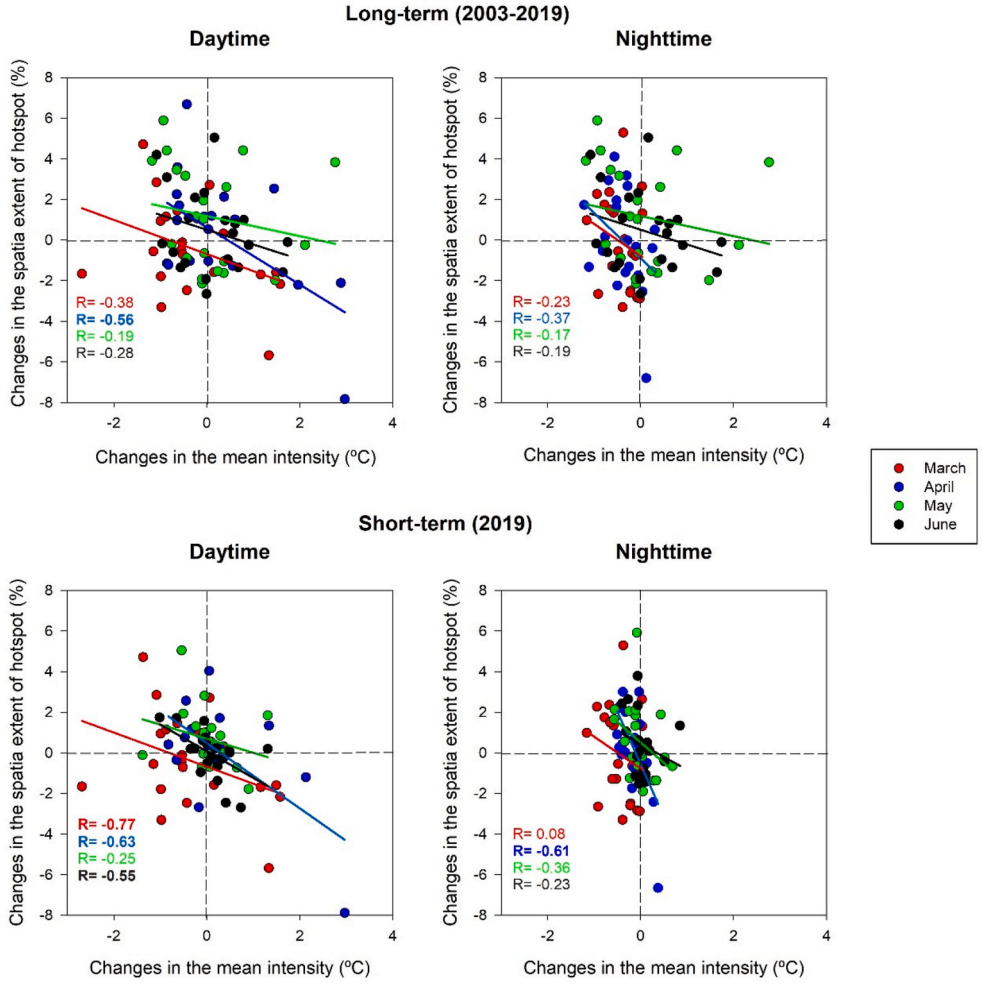

Fig. 7. Association between changes in the mean intensity of SUHI and spatial extent of hotspot area during the COVID-19 lockdown period in March–June 2020. Pearson's r correlation is computed for each month independently. Only numbers in bold are statistically significant at the 95% level ($p < 0.05$).

metropolitans like Istanbul, Tehran, and Riyadh. In these megacities, the most significant improvement in air quality corresponded mainly to deductions in CO, while SO_2 was the least improved air pollutant in these metropolitans. In this context, it is well-established that COVID-19 has altered emissions significantly, given that people spend more time at home and less time on the road (e.g. passenger vehicles, public transit, and aircraft) (Gautam, 2020a,b; Kroll et al., 2020). However, this behaviour has more influence on air pollutants like nitrogen oxide (NO_x). In our study, the impact of COVID-19 lockdown on NO_2 was more evidenced in small metropolitans and the Gulf region. This pattern may be explained by the low density of industry in these small metropolitans. It can also be linked to the notion that while measures of lockdown are country-wide rather than city-based, their application can be less restricted in megacities, mainly due to the extended agglomeration and overpopulation in these large cities. In many Gulf countries, gasoline vehicles, which emit less NOx than their diesel counterparts, are more popular, due to their better tourqe and lower consumption of fuel. In less developed countries of the Middle East, diesel vehicles are the domain of commercial vehicles, due to low income and high oil pricing. Also, the volume of gas emissions in megacities is typically larger than in small metropolitans, mainly due to intensive industrial activities, over-population, excessive energy consumption, and high traffic load. Globally, megacities consume 6.7% of the global energy, including 9.3% and 9.9% of the global electricity and gasoline, respectively (Kennedy et al., 2015). In Tehran, the annual use of energy exceeds 1000 PJ, compared to less than 500 PJ in Istanbul and Cairo (Kennedy et al., 2015). This high flow of energy in these megacities makes it difficult to recover quickly, in terms of air quality and heating intensity, during a temporary lockdown period, while small metropolitans have a "short memory" and can respond accordingly in a more efficient manner. This can be seen in the slight decrease in the mean intensity of SUHI during nighttime, when almost all human and economic activities were shut down.

Recalling the different climatic, demographic, and socioeconomic characteristics of the metropolitans employed in this study, it is expected that the SUHI characteristics would respond differently to COVID-19. This hypothesis was confirmed in this study, particularly during the daytime, where restrictive lockdown measures in most countries in the region were more relaxed than in the nighttime. Notably, a partial lockdown was imposed in the majority of the Middle East countries from March to June 2020, which began mostly in the middle or late hours of the day (mostly after 4:00 p.m. local time), implying that the effects of restrictive measures were more pronounced at night and to a lesser extent during the day. This could explain why almost all metropolitans in the region exhibited a decline in the mean intensity of their nighttime SUHI, while they exhibited either an increase or less significant decrease in the mean intensity of daytime SUHI. Overall, the decline in the mean intensity of nighttime was more pronounced in small metropolitans (e.g. Amman, Makkah, Maddinah, and Beirut) and less significant in megacities. Temporarily, we noted that the decline in the intensity of nighttime SUHI was apparent in April and May, while it was less significant in March and June. This can simply be explained by the notion that life was normal in the great course of March, with the exception of the last few

days of the month, when governments, public officials, and health authorities introduced restrictive measures to increase social distancing and control the spread of this pandemic. While more restrictions were applied in April and March, some relaxing measures were applied in June. Another explanation may relate to the fact that the response of pollutants to changes in gas emissions is delayed, in part because of previous conditions. This "memory" may explain why changes in the mean intensity of nighttime SUHI was most apparent in the majority of metropolitan cities during the middle phases of the lockdown, rather than when it began or ended.

In contrast to nighttime SUHI, a higher number of metropolitans in the Middle East showed an increase in the mean intensity of their daytime SUHI during the lockdown period, particularly in April and May. This increase was more rapid in the mega metropolitans like Tehran, Ankara, and Istanbul, as well as the Gulf metropolitans like Doha, Dubai, and Kuwait. Again, these metropolitans exhibit a high flow of energy during daytime, either due to demographic considerations (i.e. overpopulation, high traffic load, and intensive industrial activities) like megacities or excessive energy demand like the Gulf metropolitans. The only exception corresponded to Cairo, which exhibited a decline in the mean intensity of daytime SUHI. This pattern may be explained by the notion that Cairo is an urban agglomeration that represents a group of cities. Although these cities have close economic connections, they do not have a compact spatial organization, as these cities are isolated with agricultural belts in the neighbourhoods (El Kenawy et al., 2020).

It is worth noting that the lowered emissions during COVID-19 lockdown cannot only be attributed to restrictive measures. Other climatic and socioeconomic variables in the region may matter. For example, the Middle East region is characterized by high interannual variability of sand and dust storms, which bring excessive amounts of aerosols to the region (Engelstaedter et al., 2006; Middleton, 2019). The frequency of these storms is seasonally dependent, with higher frequency in winter and early spring, and less occurrence in summer and fall. These storms are associated mainly with strong synoptic-scale disturbances produced by spring cyclonic storms (Shao et al., 2010). This seasonal pattern may explain the decline in AOD and aerosols in the majority of the metropolitans during the late spring and early summer (i.e. May–June) (Mohammadpour et al., 2021). Spatially, changes in AOD and aerosols in the early spring (March and April) were generally positive (i.e. increasing) in mainland metropolitan areas of the most arid areas in the region (i.e. Arabian Peninsula, Iraq, Egypt, and Iran), which presents a major atmospheric dust sink, with high aerosol deposition rates. However, coastal metropolitans (e.g. Alexandria, Beirut, and Jeddah), located far from the tracks of these storms, exhibited less significant changes in aerosols, especially in the early spring. Similarly, the decline of other pollutants (e.g. NO_2) during the lockdown may be enhanced by some climatic configurations. This can simply be seen in the case of NO_2, which has a short chemical life span, with higher concentration levels in winter and early spring in the Northern Hemisphere (Kroll et al., 2020). The joint influence of COVID-19 and other independent variables (e.g. climate) on both air quality and SUHI characteristics is confirmed in this study in two ways. First, a comparison of SUHI characteristics during the lockdown period, based on short-term (2019) and long-term (2003–2019) anomalies, reveals that changes in SUHI characteristics were less pronounced during the lockdown when considering the short term anomaly than the long-term anomaly. This finding was evident for both the mean intensity of SUHI and the spatial coverage of hotspot area in the majority of the metropolitans in the region, especially during daytime. This implies that the impact of lockdown on SUHI characteristics cannot be seen independently from the long-term variability of climate. This is confirmed in Supplementary Figs. A3 and A.4. As illustrated, there has been a significant decrease (increase) in nighttime (daytime) LST over most of the metropolitans during the lockdown months, as compared to the long-time (2003–2019) climatology of LST. This implies that changes in SUHI characteristics during the lockdown period should also be seen in the context of a longer climate variability rather than only a short fluctuation in climate conditions due to lockdown. Globally, Yao et al. (2019) assessed trends in the intensity of SUHI for 397 big cities, suggesting a significant increase in the intensity of annual daytime SUHI across 42.1% of these cities. More recently, a similar finding was confirmed by Yao et al. (2021b) who noted that almost half of the cities in the mainland China exhibited a significant increase in the intensity of their SUHIs between 2001 and 2018.

6. Conclusions

In the Middle East, most countries imposed city-wide lockdowns and quarantine measures during 2020 in their attempts to control the spread of the COVID-19 pandemic. These measures had significant impacts on the urban systems, as they corresponded to a decrease in human activities (e.g. traffic pollution, industrial activities, catering and leisure activities, etc) and accordingly a decline in GHGs emissions. Here we provide the first assessment of the impacts of the pandemic lockdown from March to June 2020 on both air quality and SUHI characteristics in the region. The study employed satellite-based data of atmospheric pollution levels in 21 metropolitan cities to assess changes in air quality conditions during the lockdown. Results demonstrate a significant decrease in pollutants like SO_2, NO_2, and CO, mostly in the small metropolitans and to a lesser extent in megacities. Using satellite-based land surface temperature data, the study provided an assessment of changes in the mean intensity of SUHIs and spatial coverage of their hotspot areas in the region's metropolitan cities during the lockdown. Results indicate a significant reduction in the mean intensity of most of the metropolitans, especially during nighttime. This decline was more evident in small metropolitans, like Jeddah, Beirut, Muscat, and Makkah, compared to megacities in the region. It is also evident that the lockdown had less impact on daytime SUHI, especially in megacities, which experienced an increase in their mean intensity. The decline in the intensity of nighttime SUHI can be attributed to the improvement in air quality during the lockdown. However, this decrease cannot be attributed to the lockdown alone, as changes in SUHI in the region cannot be explained independently from long-term climate change in the region. It should be stressed that although this study considered a wide variety of metropolitans that span 14 countries in the Middle East, it is expected that –at the city level-there would be spatial and temporal differences in the response of city portions to COVID-19 lockdown. Indeed, these differences can be induced by the dominant land use/land cover types, population density, variations in urban form, industrial activity, and economic development level, besides relative location within the city (i.e. urban vs. sub-urban). However, consideration of these variables is a challenge in the metropolitans of the Middle East, due to the lack of a dense network of air quality measurements. Likewise, despite their high accuracy, the spatial and temporal resolution of MODIS products is still coarse to reliably monitor and diagnose all characteristics of SUHI, particularly in metropolitan areas with a wide range of environmental conditions. As SUHI is a mutual phenomenon, with complex interactions between a wide variety of physical (e.g. wind speed, relative humidity, soil properties, pollution) and anthropogenic processes, the dynamics and impacts of SUHI can vary significantly depending on the time of day and even within short distances over space (e.g. green areas, building material, sky view factor, streets width and direction, building height, etc). As such, remote sensing data at appropriate spatial scales would be needed to further explore differences in the response of urban sub-systems to this pandemic. This kind of detailed assessments can be an avenue for future research. Overall, this study can contribute to the increasing global literature on the links between COVID-19 and the air quality-urban climate nexus, focusing on a region that has received less attention in this global discussion, albeit one that is experiencing rapid urbanization and industrialization rates.

Declaration of competing interest

The authors declare that they have no known competing financial interests or personal relationships that could have appeared to influence the work reported in this paper.

Acknowledgements

Research reported in this publication was supported financially by the Ministry of Higher Education, Research, and Innovation, Oman (TRC/CRP/SQU/COVID-19/20/20) and administratively by Sultan Qaboos University, Oman. The authors are grateful to the ORNL DAAC for providing MODIS/VIIRS Land data employed in this study.

Appendix A. Supplementary data

Supplementary data to this article can be found online at https://doi.org/10.1016/j.envpol.2021.117802.

Author contributions

Ahmed M. El Kenawy: Experimental design, Database design, Data extraction and manipulation, Data visualization, Manuscript writing, Juan I. Lopez-Moreno: Experimental design, Database design, Matthew F. McCabe: Experimental design, Database design, Manuscript writing, Fernando Domínguez-Castro: Experimental design, Database design, Dhais Peña-Angulo: Experimental design, Manuscript writing, Islam M. Gaber: Experimental design, Data visualization, Abduldaem S. Alqasemi: Experimental design, Database design, Data extraction and manipulation, Khalifa M. Al Kindi: Experimental design, Database design, Data extraction and manipulation, Talal Al-Awadhi: Experimental design, Data visualization, Mohammed E. Hereher: Experimental design, Database design, Data extraction and manipulation, Sayed M. Robaa: Experimental design, Data extraction and manipulation, Noura Al Nasiri: Experimental design, Data visualization, Sergio M. Vicente-Serrano: Experimental design, Database design.

References

Abulibdeh, A., 2021. Analysis of urban heat island characteristics and mitigation strategies for eight arid and semi-arid gulf region cities. Environ. Earth Sci. 80, 1–26.
Abutaleb, K., et al., 2015. Assessment of urban heat island using remotely sensed imagery over Greater Cairo, Egypt. Adv. Rem. Sens. 4, 35.
AL Talib, B.Y., 2020. Religious tourism in Al Madina Al Munawara; and its future using GIS techniques. J. Arts Soc. Sci. 11, 1–24.
Alobaydi, D., Bakarman, M.A., Obeidat, B., 2016. The impact of urban form configuration on the urban heat island: the case study of Baghdad, Iraq. Procedia. Eng. 145, 820–827.
Alqasemi, A.S., et al., 2021. Impact of COVID-19 lockdown upon the air quality and surface urban heat island intensity over the United Arab Emirates. Sci. Total Environ. 767, 144330.
Aman, M.A., Salman, M.S., Yunus, A.P., 2020. COVID-19 and its impact on environment: improved pollution levels during the lockdown period – a case from Ahmedabad, India. Remote Sensing App.: Soc. Environ. 20, 100382.
Archer, C.L., et al., 2020. Changes in air quality and human mobility in the USA during the COVID-19 pandemic. Bull. Atmos. Sci. Technol. 1, 491–514.
Broomandi, P., et al., 2020. Impact of COVID-19 event on the air quality in Iran. Aerosal Air Q. Res. 20, 1793–1804.
Chen, Q.-X., et al., 2020. Influence of COVID-19 event on air quality and their association in Mainland China. Aerosal Air Q. Res. 20, 1541–1551.
Çiçek, İ., Doğan, U., 2006. Detection of urban heat island in Ankara, Turkey. Il Nuovo Cimento C 29, 399–409.
Costello, V.F., 1977. Urbanization in the Middle East. CUP Archive.
Dantas, G., et al., 2020. The impact of COVID-19 partial lockdown on the air quality of the city of Rio de Janeiro, Brazil. Sci. Total Environ. 729, 139085.
de Andrade, M.D., et al., 2021. Evaluation of the MOD11A2 product for canopy temperature monitoring in the Brazilian Atlantic Forest. Environ. Monit. Assess. 193, 45.
Diffenbaugh, N.S., et al., 2007. Heat stress intensification in the Mediterranean climate change hotspot. Geophys. Res. Lett. 34.
Dihkan, M., et al., 2018. Evaluation of urban heat island effect in Turkey. Arab. J. Geosci. 11, 1–20.
El-Nadry, M., et al., 2019. Urban health related air quality indicators over the Middle East and North Africa countries using multiple satellites and AERONET data. Rem. Sens. 11, 2096.
El Kenawy, A.M., et al., 2020. Nocturnal surface urban heat island over greater Cairo: spatial morphology, temporal trends and links to land-atmosphere influences. Rem. Sens. 12, 3889.
El Kenawy, A.M., et al., 2016. Recent changes in continentality and aridity conditions over the Middle East and North Africa region, and their association with circulation patterns. Clim. Res. 69, 25–43.
Elagib, N.A., 2011. Evolution of urban heat island in Khartoum. Int. J. Climatol. 31, 1377–1388.
Engelstaedter, S., Tegen, I., Washington, R., 2006. North African dust emissions and transport. Earth Sci. Rev. 79, 73–100.
Gautam, S., 2020a. COVID-19: air pollution remains low as people stay at home, *Air Quality*. Atmos. Health 13, 853–857.
Gautam, S., 2020b. The influence of COVID-19 on air quality in India: a boon or inutile. Bull. Environ. Contam. Toxicol. 104, 724–726.
Giani, P., et al., 2020. Short-term and long-term health impacts of air pollution reductions from COVID-19 lockdowns in China and Europe: a modelling study. Lancet Plantetary Health 4, e474–e482.
Ginzburg, A.S., et al., 2020. Impact of COVID-19 lockdown on air quality in Moscow. Dokl. Earth Sci. 495, 862–866.
Hashim, B.M., et al., 2021. Impact of COVID-19 lockdown on NO2, O3, PM2.5 and PM10 concentrations and assessing air quality changes in Baghdad, Iraq. Sci. Total Environ. 754, 141978.
Huang, X., Wang, Y., 2019. Investigating the effects of 3D urban morphology on the surface urban heat island effect in urban functional zones by using high-resolution remote sensing data: a case study of Wuhan, Central China. ISPRS J. Photogrammetry Remote Sens. 152, 119–131.
Imhoff, M.L., et al., 2010. Remote sensing of the urban heat island effect across biomes in the continental USA. Remote Sens. Environ. 114, 504–513.
Islam, M.S., et al., 2021. Impacts of nationwide lockdown due to COVID-19 outbreak on air quality in Bangladesh: a spatiotemporal analysis. Air Q. Atmos. Health 14, 351–363.
Jephcote, C., et al., 2021. Changes in air quality during COVID-19 'lockdown' in the United Kingdom. Environ. Pollut. 272, 116011.
Karaca, M., Anteplioğlu, Ü., Karsan, H., 1995. Detection of urban heat island in Istanbul, Turkey. Il Nuovo Cimento C 18, 49–55.
Keikhosravi, Q., 2019. The effect of heat waves on the intensification of the heat island of Iran's metropolises (Tehran, Mashhad, Tabriz, Ahvaz). Urban Climate 28, 100453.
Kennedy, C.A., et al., 2015. Energy and material flows of megacities. Proc. Natl. Acad. Sci. Unit. States Am. 112, 5985–5990.
Kroll, J.H., et al., 2020. The complex chemical effects of COVID-19 shutdowns on air quality. Nat. Chem. 12, 777–779.
Lelieveld, J., et al., 2012. Climate change and impacts in the eastern mediterranean and the Middle East. Climatic Change 114, 667–687.
Li, L., et al., 2020. Air quality changes during the COVID-19 lockdown over the Yangtze River Delta Region: an insight into the impact of human activity pattern changes on air pollution variation. Sci. Total Environ. 732, 139282.
Li, X., et al., 2017. The surface urban heat island response to urban expansion: a panel analysis for the conterminous United States. Sci. Total Environ. 605–606, 426–435.
Li, X., Fan, W., Wang, L., Luo, M., Yao, R., Wang, S., et al., 2021. Effect of urban expansion on atmospheric humidity in Beijing-Tianjin-Hebei urban agglomeration. Sci. Total Environ. 759, 144305.
Meng, Q., et al., 2018. Characterizing spatial and temporal trends of surface urban heat island effect in an urban main built-up area: a 12-year case study in Beijing, China. Remote Sens. Environ. 204, 826–837.
Middleton, N., 2019. Variability and trends in dust storm frequency on decadal timescales: climatic drivers and human impacts. Geosciences 9, 261.
Mohammadpour, K., Sciortino, M., Kaskaoutis, D.G., 2021. Classification of weather clusters over the Middle East associated with high atmospheric dust-AODs in West Iran. Atmos. Res. 259, 105682.
Mohammed, A., et al., 2020. Canopy urban heat island and its association with climate conditions in Dubai, UAE. Climate 8, 81.
Naqvi, H.R., et al., 2021. Improved air quality and associated mortalities in India under COVID-19 lockdown. Environ. Pollut. 268, 115691.
Naserikia, M., et al., 2019. The urban heat island in an urban context: a case study of Mashhad, Iran. Int. J. Environ. Res. Publ. Health 16, 313.
Nasrallah, H.A., Balling, R.C., 1993. Spatial and temporal analysis of Middle Eastern temperature changes. Climatic Change 25, 153–161.
Nassar, A.K., Blackburn, G.A., Whyatt, J.D., 2016. Dynamics and controls of urban heat sink and island phenomena in a desert city: development of a local climate zone scheme using remotely-sensed inputs. Int. J. Appl. Earth Obs. Geoinf. 51, 76–90.
Nathaniel, S., Anyanwu, O., Shah, M., et al., 2020. Renewable energy, urbanization, and ecological footprint in the Middle East and North Africa region. Environ. Sci. Pollut. Res. 27, 14601–14613. https://doi.org/10.1007/s11356-020-08017-7.
Ramahi, TM., 2010. Cardiovascular disease in the Asia Middle East region: global trends and local implications. Asia Pacific J. Public Health 22(3_suppl), 83S–89S. https://doi.org/10.1177/1010539510373034.
Rodríguez-Urrego, D., Rodríguez-Urrego, L., 2020. Air quality during the COVID-19: PM2.5 analysis in the 50 most polluted capital cities in the world. Environ. Pollut. 266, 115042.
Safarianzengir, V., et al., 2020. Monitoring, analysis and spatial and temporal zoning of air pollution (carbon monoxide) using Sentinel-5 satellite data for health management in Iran, located in the Middle East. Air Q. Atmos. Health 13, 709–719.

Shao, Y., Fink, A.H., Klose, M., 2010. Numerical simulation of a continental-scale Saharan dust event. J. Geophys. Res.: Atmosphere 115.
Shehzad, K., Sarfraz, M., Shah, S.G.M., 2020. The impact of COVID-19 as a necessary evil on air pollution in India during the lockdown. Environ. Pollut. 266, 115080.
Sibai, A. Mehio, Nasreddine, L, Mokdad, AH, Adra, N, Tabet, M, Hwalla, N, et al., 2010. Nutrition transition and cardiovascular disease risk factors in Middle East and North Africa Countries: reviewing the evidence. Ann. Nutr. Metab. 57, 193–203. https://doi.org/10.1159/000321527.
Stratoulias, D., Nuthammachot, N., 2020. Air quality development during the COVID-19 pandemic over a medium-sized urban area in Thailand. Sci. Total Environ. 746, 141320.
Tobías, A., et al., 2020. Changes in air quality during the lockdown in Barcelona (Spain) one month into the SARS-CoV-2 epidemic. Sci. Total Environ. 726, 138540.
Tonooka, H., 2005. Atmospheric correction of MODIS thermal infrared bands by water vapor scaling method. SPIE Remote Sensing. SPIE.
Tyrlis, E., et al., 2015. The role of blocking in the summer 2014 collapse of Etesians over the eastern Mediterranean. J. Geophys. Res.: Atmosphere 120, 6777–6792.
Ünal, Y.S., et al., 2020. Investigating urban heat island intensity in Istanbul. Theor. Appl. Climatol. 139, 175–190.
United Nations Population Division, U., 2018. World Urbanization Prospects.
Veefkind, J.P., et al., 2012. TROPOMI on the ESA Sentinel-5 Precursor: a GMES mission for global observations of the atmospheric composition for climate, air quality and ozone layer applications. Remote Sens. Environ. 120, 70–83.
World Health Organization, W., 2020. Novel Coronavirus (2019-nCoV): Situation Report, vol. 19. World Health Organization, Geneva.
Wu, X., Wang, L., Yao, R., Luo, M., Wang, S., Wang, L., 2020. Quantitatively evaluating the effect of urbanization on heat waves in China. Sci. Total Environ. 731, 138857.
Yao, R., et al., 2018. Interannual variations in surface urban heat island intensity and associated drivers in China. J. Environ. Manag. 222, 86–94.
Yao, R., Wang, L., Huang, X., Niu, Z., Liu, F., Wang, Q., 2017. Temporal trends of surface urban heat islands and associated determinants in major Chinese cities. Sci. Total Environ. 609, 742–754.
Yao, R., Wang, L., Huang, X., Gong, W., Xia, X., 2019. Greening in rural areas increases the surface urban heat island intensity. Geophys. Res. Lett. 46, 2204–2212. https://doi.org/10.1029/2018GL081816.
Yao, R., Wang, L., Huang, X., Wu, X., Yang, L., Niu, Z., 2021a. Assessing urbanization's contribution to warming in mainland China using satellite-estimated air temperature data. Prog. Phys. Geogr.: Earth Environ. https://doi.org/10.1177/0309133321988850.
Yao, R., Wang, L., Huang, X., Liu, Y., Niu, Z., Wang, S., et al., 2021b. Long-term trends of surface and canopy layer urban heat island intensity in 272 cities in the mainland of China. Sci. Total Environ. 772, 145607.
Zheng, Z., et al., 2019. Spatial variation of NO2 and its impact factors in China: an application of sentinel-5P products. Rem. Sens. 11, 1939.
Zhou, D., Bonafoni, S., Zhang, L., Wang, R., 2018. Remote sensing of the urban heat island effect in a highly populated urban agglomeration area in East China. Sci. Total Environ. 628–629, 415–429.